Article:
do Nascimento, Júlio César A., Kerrigan, Adam, Hasnip, Philip J. orcid.org/0000-0002-4314-4093 et al. (1 more author) (2022) Significant improvement of the Seebeck coefficient of Fe2VAl with antisite defects. Materials Today Communications. 103510. ISSN: 2352-4928

https://doi.org/10.1016/j.mtcomm.2022.103510

Materials Today Communications 31 (2022) 103510

Contents lists available at ScienceDirect

Materials Today Communications

journal homepage: www.elsevier.com/locate/mtcomm

Significant improvement of the Seebeck coefficient of Fe_2VAl with antisite defects

Júlio César A. do Nascimento, Adam Kerrigan, Philip J. Hasnip, Vlado K. Lazarov *

University of York, United Kingdom

ARTICLE INFO

Keywords:
Thermoelectrics
Seebeck coefficient
Point defects
Heusler material

ABSTRACT

In this work we present first principles study of the effect of stoichiometric pairs of antisite defects, V occupying Al site (V_{Al}) and Al occupying V site (Al_V), on the electronic structure and Seebeck coefficient of the Fe_2VAlHeusler alloy. We show that introduction of these defects opens the bandgap of Fe_2VAl, changing it from semi-metal to semiconductor, which results in an increase of the Seebeck coefficient for a range of doping concentrations and temperatures. We calculated Seebeck coefficients at different doping concentrations and temperatures shows good agreement with experimental data.

1. Introduction

Improving the efficiency of our energy usage is one of the steps required to solve number of energy related problems the world is facing currently. Moreover industrial processes, transport, household appliances, etc. are well known sources of heat waste. Hence harvesting this heat waste is rather important to address global issues such as climate change. Thermoelectric materials can play a major role in the improvement of energy efficiency, in all temperature ranges [1]. These materials possess the unique ability to convert a temperature difference into electricity or vice versa without mechanical moving parts. Providing excellent opportunities for harvesting waste heat [2–6].

Current thermoelectric devices found in the market rely on Bi–Te based materials, although it shows marketable efficiency, its widespread application are limited since they are not earth-abundant materials [7,8].

Hence materials systems that are based on abundant elements are of particular interest for thermoelectric applications. $Fe_2VAl$is a material system that has attracted a great deal of attention due to its potentials as a thermoelectric [7]. Fe_2VAlhas higher power factor compared to Bi–Te based thermoelectrics, although due to its higher thermal conductivity the figure of merit ZT is significantly lower than that of Bi–Te based materials. In the past significant experimental efforts have been made to improve the ZT of $Fe_2VAl$by nanostructuring [9], for example, by introducing point defects in the pristine structure of Fe_2VAl. Among the possible point defects that can occur some of the most energetically favourable are the antisite defects V_{Al}, and Al_V [10].

In this work, we use first principle calculations to evaluate how the presence of stoichiometric pairs of V_{Al}, and Al_V antisites, as an Al/V inversion defects changes the thermoelectric properties of Fe_2VAl, specifically the Seebeck coefficient and its temperature dependence. We also compare the results with experimental data available in the literature [11–15], and predict Seebeck coefficient trends and magnitude as a function of the concentration of point defects.

2. Methods

The Fe_2VAlfalls in the group of Heusler alloys, which have the chemical formula X_2YZ, where X and Y are transition metals and Z is a p-block element. The structure of $Fe_2VAl$is face-centred cubic, with space group $Fm\bar{3}m$ (225). There are four Fe_2VAlformula units (f.u.) in the cubic unit cell, i.e. 16 atoms in the unit cell. A primitive rhombohedral unit cell contains 1 f.u., this reduces the number of atoms to 4, hence it is more convenient to be used for computational reasons, Fig. 1. In the rhombohedral cell, the Fe atoms fractional coordinates are (1/4, 1/4, 1/4) and (3/4, 3/4, 3/4), while Al and V are at (1/2, 1/2, 1/2) and (0, 0, 0), respectively. In order to include the defects in a low concentration we have constructed supercells based on Fe_2VAlrhombohedral cell. To introduce the inversion defects we implemented a 3 × 3 × 3 supercell. The lowest energy arrangement for a sequence of inversion defects is to have them formed around one of the Fe atoms [16]. Fig. 2 shows the position of the defects with respect to the rhombohedral supercell we highlight the cubic unit cell embedded in the supercell, . The size of the chosen supercell allows us to simulate antisite defects with concentrations of 2/57, 4/57, 6/57 and 8/57, which represents the fraction of V and Al atoms that are forming the inversion defects.

* Corresponding author.
E-mail addresses: jcdn500@york.ac.uk (J.C. do Nascimento), vlado.lazarov@york.ac.uk (V.K. Lazarov).

https://doi.org/10.1016/j.mtcomm.2022.103510
Received 2 January 2022; Received in revised form 4 April 2022; Accepted 5 April 2022
Available online 21 April 2022

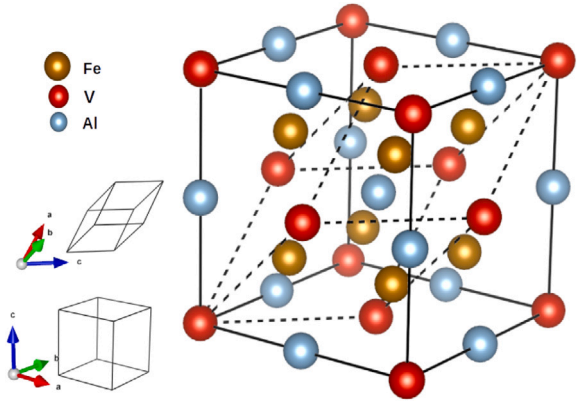

Fig. 1. Schematic of the cubic and rhombohedral (dashed lines) possible unit cells of Fe_2VAlunit cell.

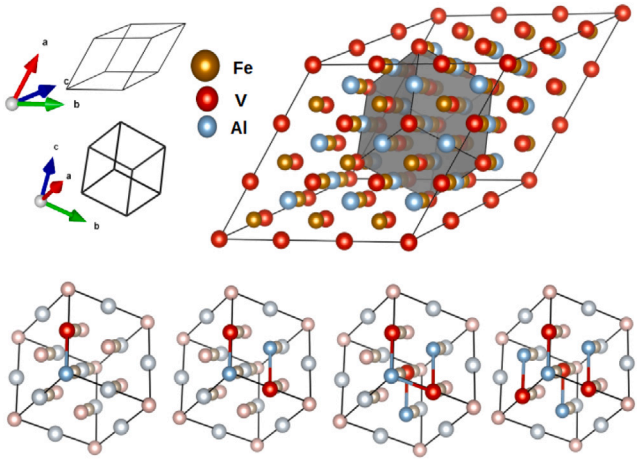

Fig. 2. Schematics of the rhombohedral supercell used in the calculations, the cubic structure is outlined.

We performed first-principles calculations using the CASTEP [17] code with the GGA-PBE exchange–correlation functional [18], using plane-wave cut-off energy of 800 eV with a grid-scale of size 2.0 and a fine grid scale of size 3.0, that was necessary to ensure that the calculation agrees with the variational principle. The Brillouin zone was sampled using a Monkhorst–Pack [19] grid with a 5 × 5 × 5 k-points mesh, for the 3 × 3 × 3 supercells. On-the-fly ultrasoft pseudopotentials (C19 set) were used. The structure was fully optimized until pressure and energy were converged to 0.01 GPa and 0.02 meV/atom, respectively.

We calculated the transport properties using the semi-classical Boltzmann transport formalism within the constant relaxation time approximation as implemented in the BoltzTraP2 code [20].

3. Results

First we present the calculations of Seebeck coefficient as a function of concentration of antisite defects. Fig. 3 shows calculated Seebeck coefficients for 3.7%, 7.4%, 11.11% and 16.6% antisite defect concentrations and pristine structure. Calculated values of the Seebeck coefficients with respect to charge carriers are compared to experimental values found in the literature, where modulation of the charge carriers in $Fe_2VAl$is obtained by doping with Si, Ir and Ti, where x represent the percentage of doping element [11–14]. The defect percentages refer to the number of the total of V and Al atoms that participate in the swap defects.

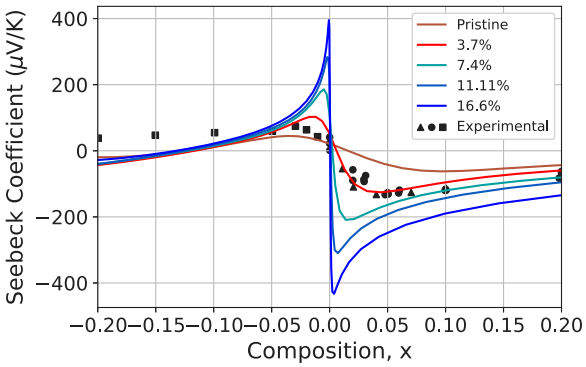

Fig. 3. Seebeck coefficient against doping composition, were $Fe_2VAl_{1-x}Si_x$ (circles) and $Fe_{2-x}VAlIr_x$ (triangles), are used for the n-type side (positive composition) and $Fe_2V_{1-x}Ti_xAl$ (squares), is used for the p-type side (negative composition), all results are for 300 K.

We can see that the calculated results show a good agreement with the experimental data for a V/Al substitution rate of around 3.7%, for the n type of doping, e.g. the maximum values of the Seebeck peak and its dependence on the composition (x) match well. On the other hand there is a small discrepancy between calculated results to the experimental data on the p-doped side. This indicates that different dopants concentration may effect the antisite defects formation energies, hence variations of Seebeck coefficient as a function of the carriers concentration.

Next we follow the trend and magnitude of Seebeck coefficient by increasing the defect concentrations. The increase of the defect concentration results in a higher peak for the Seebeck coefficient. This comes from the tendency of the antisite defects to turn $Fe_2VAl$from a semimetal to a small gap semiconductor as illustrated in Fig. 4. The Figs. 4(a–c) shows the evolution of band structure of Fe_2VAlas a function of a concentration of the antisite defects. As can be seen in Fig. 4(a) the pristine Fe_2VAlhas semimetal states and as concentration increases (from 3.7% to 16.6%) a sizable band gap opens. As expected, this trend has a negative effect on the electrical conductivity as depicted in Fig. S1 in the supplemental information. Previous reports have discussed a gap opening by introduction of different exchange–correlation functionals such as meta-GGA mBJ [21] and the hybrid functional B1-WC [22], and also by the inclusion of Hubbard U potentials [23]. In addition, our calculations capture the asymmetry of the Seebeck coefficient for n and p-type doping which is present in experimental results. However this effect is not present in calculations when defects are not considered (see Fig. 3 for pristine cell).

Next we evaluate how the antisite defects affect the Seebeck coefficient of $Fe_2VAl$for different ranges of temperatures, i.e. temperature dependence of Seebeck coefficient. The results are presented as heatmaps that graphically show the variation of the calculated Seebeck coefficient for a range of compositions and temperatures, for 3.7%, 7.4%, 11.11% and 16.6% antisite defect concentrations and pristine structure, Fig. 5(a–d). Within the temperature range between 100 K and 500 K Seebeck coefficient has the highest value, as shown by the sharp change in colour from blue to red, where the blue region (i.e. negative of x axis) corresponds to p-type doping and the red region (positive x-axis) to n-type doping. For the temperatures above 500 K for all defects concentrations the Seebeck coefficient decreases and its variation with carrier concentrations is smaller than the lower by 500 K temperatures. Another important finding is that the maximum of the Seebeck coefficient increases with the increase of defect concentration, and the maxima are moving towards the zero of the composition axis (x-axis), as seen by the sharpness of colour change from blue to red, which is particularly sharp in Fig. 5(c–d). This show that the increase of defects increases the thermoelectric conversion capability of Fe_2VAl, and more importantly reduces the amount of doping required for an optimum

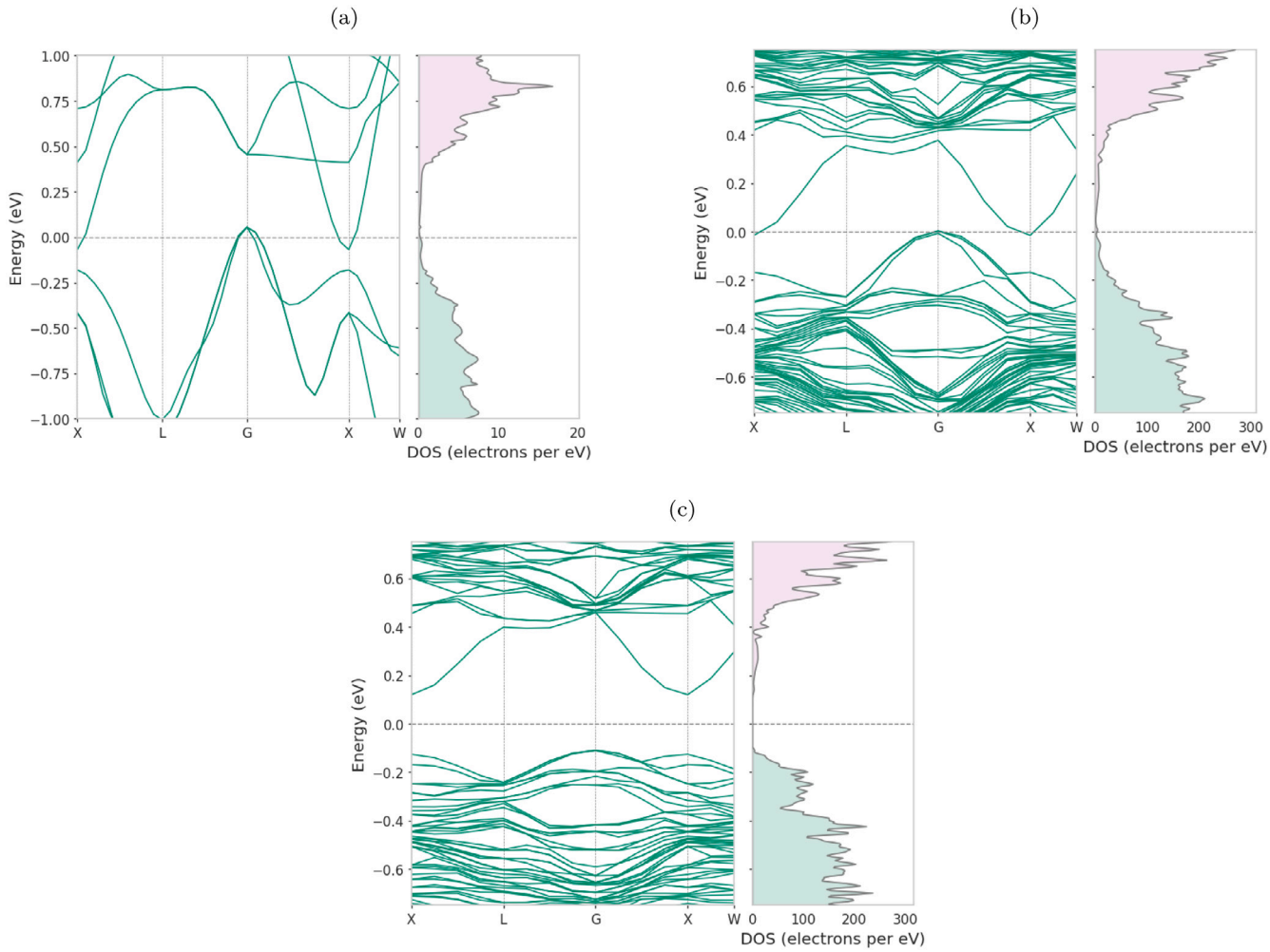

Fig. 4. Bandstructure and density of states plot of Fe_2VAl, for (a) pristine and (b) 3.7% and (c) 16.6% of Al/V inversion defects. The energy axis corresponds to E-E_F, where E_F is the Fermi energy.

Seebeck coefficient in the range of medium temperatures (300 K–600 K). In order to make comparison of these results with experimental data for Fe_2VAlavailable in the literature, in Fig. 5(e) we show the calculated Seebeck coefficient of $Fe_2VAl$for different antisite defects concentrations, starting from pristine to 16.6% defects concentrations, as well as experimental data from x=0 and x=0.05 [11,14,15]. A very good agreement with experimental data is found in both cases with presence of 3.7% of inversion defects, for a range of temperatures. For the case of a doping composition of x=0.05 in Fig. 5(f) again we have a remarkable agreement between the calculated values and the experimental data. These comparison validates the overall conclusion and results based on the undertaken calculations.

4. Conclusion

In summary, by using first principle calculations we have shown that the band gap of Fe_2VAlopens with the introduction of antisite stoichiometric disorder on the V/Al sublattice, changing it from a semimetal to a semiconductor. This leads to a sharp increase of the maximum value of the Seebeck coefficient, which is proportional to the concentration of the antisite defects. The presence of antisite defects suppress the level of doping required to increase the Seebeck coefficient maxima. The calculations performed at different temperatures show that for all concentrations of antisite defects, Fe_2VAlhas a higher Seebeck coefficient for the temperatures between 100 K–500 K. In addition, the calculated Seebeck coefficients are in good agreement with the experimental data in the literature, when comparison was done for range of compositions and temperatures. This work show that the inclusion of disorder in the V/Al sublattice is a potential pathway to increase the power factor of Fe_2VAl, by tuning both the inversion defects and doping concentrations.

Declaration of competing interest

The authors declare that they have no known competing financial interests or personal relationships that could have appeared to influence the work reported in this paper.

Acknowledgements

This project was undertaken on the Viking Cluster, which is a high performance compute facility provided by the University of York. We are grateful for computational support from the University of York High Performance Computing service, Viking and the Research Computing team".

Appendix A. Supplementary data

Supplementary material related to this article can be found online at https://doi.org/10.1016/j.mtcomm.2022.103510.

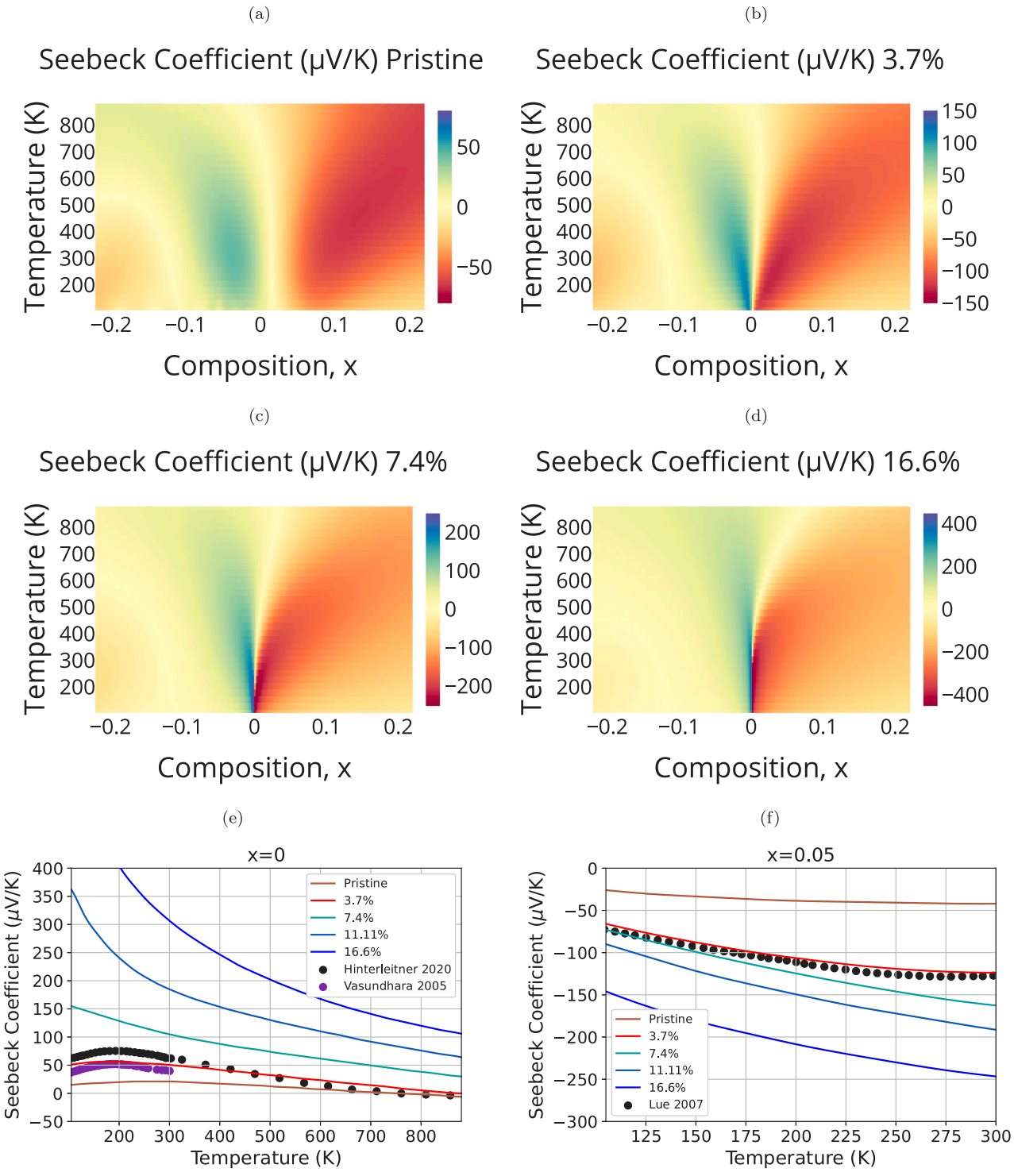

Fig. 5. Heatmap plots of the composition and temperature for pristine (a), and Al/V inversion defect concentrations of 3.7% (b), 7.4% (c) and 16.6% (d). Seebeck coefficient against temperature compared with literature experimental values [11,14,15], in the figures (e) and (f).

References

[1] Jiangtao Wei, Liangliang Yang, Zhe Ma, Peishuai Song, Mingliang Zhang, Jing Ma, Fuhua Yang, Xiaodong Wang, Review of current high-ZT thermoelectric materials, J. Mater. Sci. 55 (27) (2020) 12642–12704.

[2] Sarah Brückner, Selina Liu, Laia Miró, Michael Radspieler, Luisa F. Cabeza, Eberhard Lävemann, Industrial waste heat recovery technologies: An economic analysis of heat transformation technologies, Appl. Energy 151 (2015) 157–167.

[3] Mohamed Fathi Sanad, Ahmed Esmail Shalan, Sameh O. Abdellatif, Esraa Samy Abu Serea, Mina Shawky Adly, Md. Ariful Ahsan, Thermoelectric energy harvesters: A review of recent developments in materials and devices for different potential applications, Top. Curr. Chem. 378 (6) (2020).

[4] Mohamed Amine Zoui, Saïd Bentouba, John G. Stocholm, Mahmoud Bourouis, A review on thermoelectric generators: Progress and applications, Energies 13 (14) (2020).

[5] Hussam Jouhara, Navid Khordehgah, Sulaiman Almahmoud, Bertrand Delpech, Amisha Chauhan, Savvas A. Tassou, Waste heat recovery technologies and applications, Therm. Sci. Eng. Prog. 6 (2018) 268–289.

[6] Ling Xu, Matthew P. Garrett, Bin Hu, Doping effects on internally coupled seebeck coefficient, electrical, and thermal conductivities in aluminum-doped TiO2, J. Phys. Chem. C 116 (24) (2012) 13020–13025.

[7] Yoshiki Takagiwa, Yoshikazu Shinohara, A practical appraisal of thermoelectric materials for use in an autonomous power supply, Scr. Mater. 172 (2019) 98–104.
[8] Robert Freer, Anthony V. Powell, Realising the potential of thermoelectric technology: a roadmap, J. Mater. Chem. C 8 (2) (2020) 441–463.
[9] Eric Alleno, Review of the thermoelectric properties in nanostructured Fe2VAl, Metals 8 (11) (2018).
[10] Subrahmanyam Bandaru, Philippe Jund, Electronic structure of the Heusler compound Fe2VAl and its point defects byab initiocalculations, Phys. Status Solidi (B) 254 (2) (2016) 1600441.
[11] M. Vasundhara, V. Srinivas, V.V. Rao, Low-temperature electrical transport in Heusler-type Fe2V (AlSi) alloys, J. Phys.: Condens. Matter 17 (38) (2005) 6025–6036.
[12] M. Vasundhara, V. Srinivas, V.V. Rao, Electronic transport in Heusler-typeFe2VAl1-xMxalloys(M=B, In, Si), Phys. Rev. B 77 (22) (2008).
[13] Y. Nishino, Y. Tamada, Doping effects on thermoelectric properties of the off-stoichiometric Heusler compounds Fe2-xV1+xAl, J. Appl. Phys. 115 (12) (2014) 123707.
[14] C.S. Lue, C.F. Chen, J.Y. Lin, Y.T. Yu, Y.K. Kuo, Thermoelectric properties of quaternary Heusler alloysFe2VAl1-xSix, Phys. Rev. B 75 (6) (2007).
[15] B. Hinterleitner, P. Fuchs, J. Rehak, F. Garmroudi, M. Parzer, M. Waas, R. Svagera, S. Steiner, M. Kishimoto, R. Moser, R. Podloucky, E. Bauer, Stoichiometric and off-stoichiometric full Heusler Fe2V1-xWxAl thermoelectric systems, Phys. Rev. B 102 (7) (2020).
[16] A. Berche, M.T. Noutack, M.-L. Doublet, P. Jund, Unexpected band gap increase in the Fe2VAl Heusler compound, Mater. Today Phys. 13 (2020) 100203.
[17] Stewart J. Clark, Matthew D. Segall, Chris J. Pickard, Phil J. Hasnip, Matt I.J. Probert, Keith Refson, Mike C. Payne, First principles methods using CASTEP, Z. Kristallogr. Cryst. Mater. 220 (5–6) (2005) 567–570.
[18] John P. Perdew, Kieron Burke, Matthias Ernzerhof, Generalized gradient approximation made simple, Phys. Rev. Lett. 77 (1996) 3865–3868.
[19] Hendrik J. Monkhorst, James D. Pack, Special points for brillouin-zone integrations, Phys. Rev. B 13 (1976) 5188–5192.
[20] Georg K.H. Madsen, Jesús Carrete, Matthieu J. Verstraete, BoltzTraP2, a program for interpolating band structures and calculating semi-classical transport coefficients, Comput. Phys. Comm. 231 (2018) 140–145.
[21] Shamim Sk, P. Devi, Sanjay Singh, Sudhir K. Pandey, Exploring the best scenario for understanding the high temperature thermoelectric behaviour of Fe2VAl, Mater. Res. Express 6 (2) (2018) 026302.
[22] Daniel I. Bilc, Philippe Ghosez, Electronic and thermoelectric properties of Fe2VAl: The role of defects and disorder, Phys. Rev. B 83 (20) (2011).
[23] G.A. Naydenov, P.J. Hasnip, V.K. Lazarov, M.I.J. Probert, Effective modelling of the seebeck coefficient of Fe2VAl, J. Phys.: Condens. Matter 32 (12) (2019) 125401.